

Two-dimensional energy bands at the $\text{CaF}_2/\text{Si}(111)$ interface

F. J. Himpsel, T. F. Heinz, A. B. McLean, and E. Palange

IBM Research Division, T. J. Watson Research Center, Box 218, Yorktown Heights, New York 10598

E. Burstein

Department of Physics, University of Pennsylvania, Philadelphia, Pennsylvania 19104-6396

(Received 8 February 1989; accepted 7 April 1989)

We have chosen $\text{CaF}_2/\text{Si}(111)$ as a prototype to study the two-dimensional band structure of an ordered interface using angle-resolved photoemission and optical second harmonic generation. A pair of interface state bands is found, one occupied, the other empty. The former disperses from $E_F - 0.8$ eV at Γ to $E_F - 1.4$ eV (-1.6 eV) at M (K). An interface band gap of 2.4 eV is determined via resonant second harmonic generation using a truly buried interface with 500 Å of CaF_2 on top of Si. Therefore, the interfacial gap is twice as large as the gap in Si and five times smaller than the gap in CaF_2 . The pair of interface bands can be understood as bonding/antibonding combinations of the Si dangling bond orbital and the Ca $4s$ orbital, with Ca in the $1+$ oxidation state.

I. INTRODUCTION

So far, the electronic structure of interfaces has been explored much less than the electronic structure of surfaces. One reason for this is the difficulty in obtaining a strong signal from the interface. One usually finds a large background from the substrate and the overlayer. The substrate signal can be suppressed by choosing a technique with a very short probing depth (e.g., scanning tunneling spectroscopy or atom scattering). However, these probes have difficulty penetrating overlayers. This problem can be solved in various ways. Optical methods have good penetration and can be made sensitive to the interface by taking advantage of dipole selection rules. For example, optical second harmonic generation occurs only in the absence of inversion symmetry. We will demonstrate the application of this method and others for determining the two-dimensional electronic structure of a model interface, namely $\text{CaF}_2/\text{Si}(111)$.

The $\text{CaF}_2/\text{Si}(111)$ interface¹ is a prime test case for this purpose since the nature of the bonding changes across the interface from covalent to ionic. Consequently, the properties of the interface layer are quite different from those of either Si or CaF_2 . For example, the band gap of the interface layer is found to be twice as large as that of Si (and five times smaller than that of CaF_2), indicating some kind of intermediate bonding configuration.

II. OCCUPIED INTERFACE BAND BY PHOTOEMISSION

An interface state can be identified by several means. In photoemission experiments²⁻¹² its intensity is attenuated with increasing overlayer thickness due to the finite escape depth of the photoelectrons (~ 5 Å). However, relative to the substrate, its intensity remains constant. This is demonstrated for the $\text{CaF}_2/\text{Si}(111)$ interface in Fig. 1. The spectra are taken for several coverages of CaF_2 (1 L corresponds to a F-Ca-F triple layer with 3.15-Å thickness). They cover the valence band region of Si and CaF_2 . The upper edge of the

F $2p$ -like valence band of CaF_2 lies ~ 8.5 eV below that of Si, which has mostly Si $3p$ character. About 1.5 eV below the valence band edge of Si there is an interface state (tickmarks in Fig. 1), which is not present on the clean $\text{Si}(111)7\times 7$ surface, but exists for all CaF_2 coverages. Its intensity remains constant relative to the Si valence band emission with increasing CaF_2 coverage, but decreases in absolute terms. Note that the CaF_2 valence band undergoes interesting line-shape changes with film thickness. For one layer of CaF_2 there is a single peak, whereas for more than one layer a second component appears at lower energy, probably reflecting the transition from a two-dimensional to a three-dimensional solid.

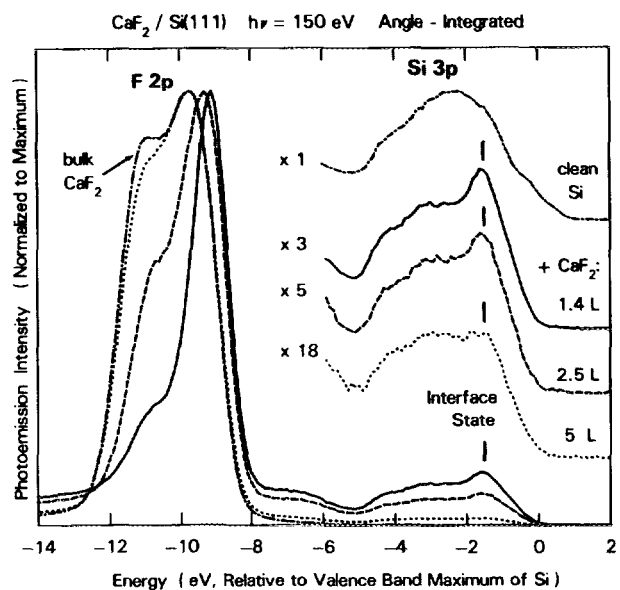


FIG. 1. Overview photoelectron spectra showing the valence bands of Si and CaF_2 and the interface state (after Ref. 8). The latter is identified by its intensity, which is attenuated with increasing thickness of CaF_2 but remains constant relative to the Si substrate (1 L = one F-Ca-F triple layer = 3.15 Å.)

In order to obtain a complete description of this interface state, all of its quantum numbers have to be determined, i.e., the two-dimensional energy-versus-momentum band dispersion $E(k_{\parallel})$ and the point group symmetry. This can be done using angle-resolved, polarization dependent photoemission¹² (Figs. 2 and 3). Hereby one has a further opportunity to test the two-dimensional character of this state. If it were three-dimensional, one would expect a band dispersion in the direction perpendicular to the interface, which can be mapped by changing the photon energy at fixed k_{\parallel} . Such a dispersion is not found,¹² confirming the two-dimensional character of this state. As the band structure plot (Fig. 3) indicates, there are no three-dimensional bulk states available at the Brillouin zone boundary (M, K) that could hybridize with the interface state. At the zone center (Γ), however, such states do exist. They broaden and weaken the interface state, but do not quench it altogether. Apparently, the overlap between bulk and interface states is small for such a heterogeneous interface. In metal-metal interfaces, where interface states have been identified at particular k_{\parallel} points, this overlap is much stronger and makes the determination of the interface state dispersion over the entire Brillouin zone difficult, if not impossible.

The remaining quantum number, i.e., the point group symmetry, is obtained by using polarization selection rules (Fig. 2). For example, at $k_{\parallel} = 0(\Gamma)$ the point group is C_{3v} , and the states of Λ_1 symmetry are seen with the electric field vector \mathbf{E} perpendicular to the surface, whereas Λ_3 states are seen with \mathbf{E} parallel to the interface (Λ_2 states cannot be seen in normal emission). Experimentally, one finds¹² Λ_1 symmetry, which corresponds to s, p_z type orbitals.

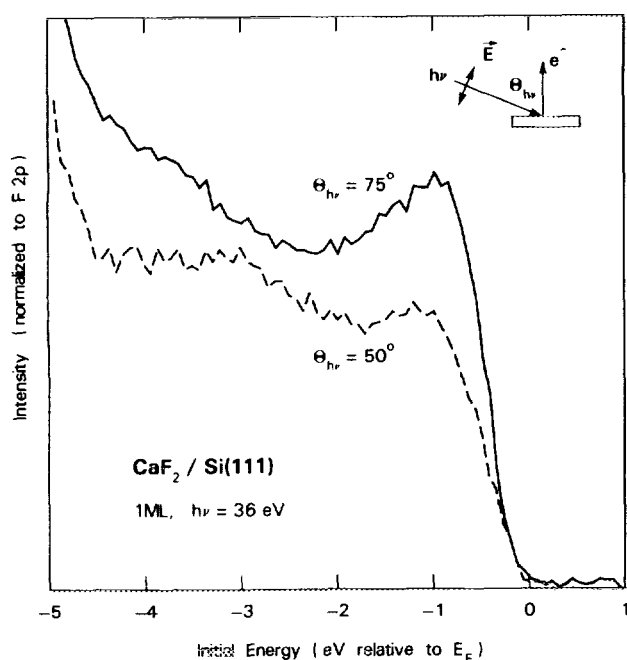


FIG. 2. Polarization-dependent photoelectron spectra from $\text{CaF}_2/\text{Si}(111)$ in normal emission. The intensity of the interface state (at about -1 eV) for the two polarizations is consistent with excitation by the component of the electric field vector \mathbf{E} normal to the surface. From dipole selection rules it follows that the state has Λ_1 symmetry.

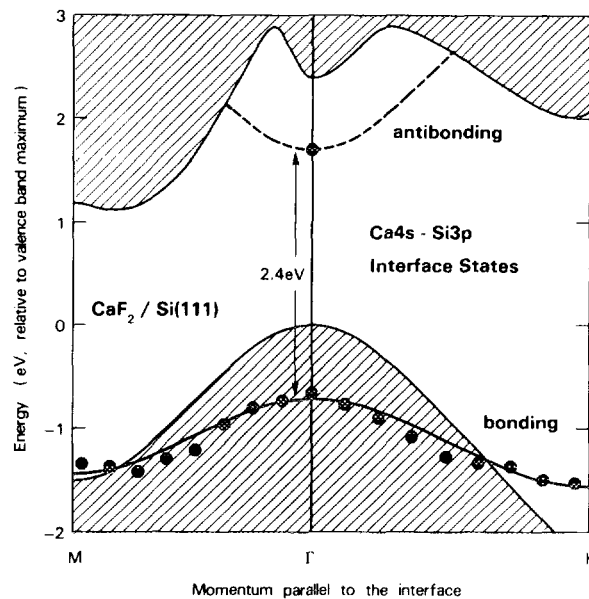


FIG. 3. $E(k_{\parallel})$ band dispersion for interface states on $\text{CaF}_2/\text{Si}(111)$. The occupied band is obtained from photoemission (Fig. 2), the bottom of the unoccupied band from optical second harmonic generation (Fig. 4), and the dispersion of the unoccupied band is estimated from a band calculation (Ref. 20) for the isoelectronic $\text{Na}/\text{Si}(111)$ system. The hatched regions represent bulk bands of Si.

A simple picture of the electronic structure at the $\text{CaF}_2/\text{Si}(111)$ interface arises if one starts from the orbitals that form the bond across the interface.^{5,6} The $\text{Si}(111)$ surface has one half-filled broken bond orbital per atom with predominantly Si $3p$ character. According to core level measurements^{5,6} the Ca atoms in the layer adjacent to Si have changed their oxidation state from $2+$ to $1+$. This change in oxidation state creates a single Ca $4s$ electron, which can pair with the Si $3p$ broken bond electron to form the interface bond. The bonding produces the occupied interface state that is seen in photoemission. Its average energy is lowered by 1.3 eV relative to the Fermi level, where the non-interacting half-filled orbitals would reside. This represents the energy that each Si and each Ca interface atom gains by bonding across the interface. Of course, there are other energies that will partially offset this gain, e.g., the energy to remove a layer of fluorine from the interface and create a Ca-terminated interface.⁷ By removing fluorine from the interface as neutral F° , an electron is left behind which converts Ca^{2+} to Ca^{1+} . Structure determinations of the $\text{CaF}_2/\text{Si}(111)$ interface¹³⁻¹⁵ are consistent with this picture as long as one considers only the Ca-terminated interface that is obtained^{7,8} after annealing close to the desorption point of the CaF_2 . There is disagreement on whether Ca is located in the covalent on-top site or in the ionic hollow site, like in CaSi_2 . For our qualitative picture the actual site of the Ca atom is irrelevant.

III. INTERFACE BAND GAP FROM OPTICAL SECOND HARMONIC GENERATION

The simple bonding picture put forward in the previous paragraph requires an unoccupied, antibonding counterpart

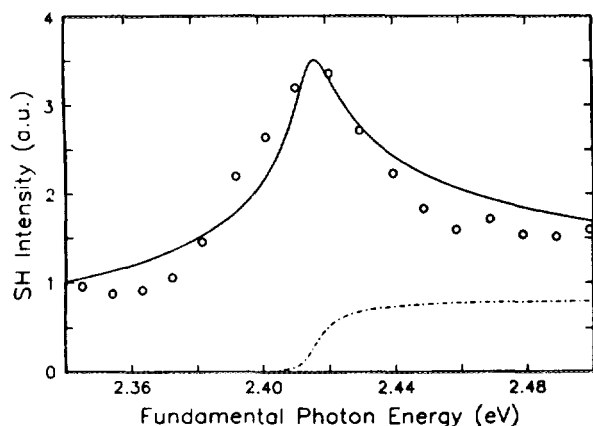


FIG. 4. Optical second harmonic intensity vs incident photon energy $h\nu$ for $\text{CaF}_2/\text{Si}(111)$ (O; after Ref. 17). The onset of interband transitions at the interface at $h\nu = 2.4$ eV is modeled by the square of the second order susceptibility (—) with a steplike imaginary part (---).

to the interface state seen in photoemission. One might look for this state using inverse photoemission. However, the extreme sensitivity of CaF_2 to radiation damage¹¹ makes such an experiment nearly impossible. Another possibility would be two-photon photoemission, provided the lifetime in the unoccupied interface state is long enough to build up a significant population. For CaF_2 films in the monolayer regime such a state has been seen with scanning tunneling spectroscopy.¹⁶ We have chosen an optical experiment, i.e., second harmonic generation, to detect the onset of interband transition across the band gap that is formed between the bonding and antibonding interface states.¹⁷

The reason for choosing optical second harmonic generation as an interface probe is due to the fact that it occurs only at the interface, where the inversion symmetry is broken, and not in the centrosymmetric bulk media (Si and CaF_2). This selectivity of second harmonic generation (and sum frequency generation in general) can be explained by simple quadratic response theory. The electric polarization \mathbf{P} induced at the sum frequency $\omega_3 = \omega_1 + \omega_2$ is related to the electric field strengths \mathbf{E} at ω_1 and ω_2 by a quadratic susceptibility χ ,

$$\mathbf{P}(\omega_3) = \chi:\mathbf{E}(\omega_1)\mathbf{E}(\omega_2).$$

Therefore χ is a third rank tensor. Under inversion, the vectors $\mathbf{P}(\omega_3)$, $\mathbf{E}(\omega_1)$, $\mathbf{E}(\omega_2)$ change sign; hence, χ must change its sign. On the other hand, χ has to remain unaffected by inversion for an inversion-symmetric medium. Consequently, $\chi = 0$ is the only possible solution.

In Fig. 4 the intensity of the second harmonic is monitored while tuning the fundamental frequency across the interface band gap E_g . As soon as interband transition become possible, the second harmonic intensity is resonantly enhanced. To ensure that the resonance occurs at $\hbar\omega = E_g$ and not at $2\hbar\omega = E_g$ we have used several combinations of frequencies (not shown, see Ref. 17). The second harmonic response does not follow the steplike joint density of states (dot-dash in Fig. 4) directly, because both the imaginary part and the

real part of χ contribute to the second harmonic signal. This can be modeled as shown in Fig. 4 (full line).

IV. SUMMARY AND OUTLOOK

Using $\text{CaF}_2/\text{Si}(111)$ as a prototype, it has been demonstrated that the two-dimensional band structure of an interface can be determined. A simple interpretation of the interface states has been given in terms of bonding and antibonding combinations of half-filled orbitals. Clearly, it would be desirable to further quantify this picture by first principles band calculations, and these have just begun for this interface.¹⁸⁻²⁰ The change in the band gap that is found at the interface shows that the electronic properties of the interface may differ strongly from the bulk properties of either solid. Such observations suggest that new materials may be engineered by producing structures with a large density of interfaces, e.g., superlattices with periods of a few atomic layers.

¹For an overview of possible applications of CaF_2/Si epitaxial layers, see *Proceedings of the Second International Symposium on Silicon Molecular Beam Epitaxy*, edited by John C. Bean and Leo J. Schowalter (The Electrochemical Society, Pennington, NJ, 1988), Vol. 88-8; in particular, see articles by Julia M. Phillips and L. Pfeiffer, p. 129; L. J. Schowalter and F. W. Fathauer, p. 140; H. Ishiwara, H. C. Lee, S. Kanemaru, and S. Furukawa, p. 182; and H. Zogg, S. Blunier, and J. Masek, p. 321.

²F. J. Himpfel, F. U. Hillebrecht, G. Hughes, J. L. Jordan, U. O. Karlsson, F. R. McFeely, J. F. Morar, and D. Rieger, *Appl. Phys. Lett.* **48**, 596 (1986).

³U. O. Karlsson, F. J. Himpfel, J. F. Morar, D. Rieger, and J. A. Yarmoff, *J. Vac. Sci. Technol. B* **4**, 1117 (1986).

⁴M. A. Olmstead, R. I. G. Uhrberg, R. D. Bringans, and R. Z. Bachrach, *J. Vac. Sci. Technol. B* **4**, 1123 (1986).

⁵F. J. Himpfel, U. O. Karlsson, J. F. Morar, D. Rieger, and J. A. Yarmoff, *Phys. Rev. Lett.* **56**, 1497 (1986).

⁶D. Rieger, F. J. Himpfel, U. O. Karlsson, F. R. McFeely, J. F. Morar, and J. A. Yarmoff, *Phys. Rev. B* **34**, 7295 (1986).

⁷M. A. Olmstead, R. I. G. Uhrberg, R. D. Bringans, and R. Z. Bachrach, *Phys. Rev. B* **35**, 7526 (1987).

⁸F. J. Himpfel, U. O. Karlsson, J. F. Morar, D. Rieger, and J. A. Yarmoff, *Mat. Res. Soc. Symp. Proc.* **94**, 181 (1987).

⁹M. A. Olmstead and R. D. Bringans, *Mater. Res. Soc. Symp. Proc.* **94**, 195 (1987).

¹⁰S. J. Morgan, A. R. Law, and R. H. Williams, *Vacuum* **38**, 381 (1988).

¹¹U. O. Karlsson, F. J. Himpfel, J. F. Morar, F. R. McFeely, D. Rieger, and J. A. Yarmoff, *Phys. Rev. Lett.* **57**, 1247 (1986).

¹²A. B. McLean and F. J. Himpfel, *Phys. Rev. B* **39**, 1457 (1989).

¹³F. A. Ponce, G. B. Anderson, M. A. O'Keefe, and L. J. Schowalter, *J. Vac. Sci. Technol. B* **4**, 1121 (1986).

¹⁴J. L. Batstone, J. M. Philips, and E. C. Hunke, *Phys. Rev. Lett.* **60**, 1394 (1988); R. M. Tromp, F. K. LeGoues, W. Kralow, and L. J. Schowalter, *ibid.* **61**, 2274 (1988); J. L. Batstone and J. M. Philips, *ibid.* **61**, 2275 (1988).

¹⁵R. M. Tromp and M. C. Reuter, *Phys. Rev. Lett.* **61**, 1756 (1988).

¹⁶Ph. Avouris and R. Wolkow, *Mat. Res. Soc. Symp. Proc.* **131**, 157 (1989) and *Appl. Phys. Lett.*, submitted.

¹⁷E. Palange, T. F. Heinz, F. J. Himpfel, and E. Burstein, *Bull. Am. Phys. Soc.* **33**, 298 (1988). T. F. Heinz, F. J. Himpfel, E. Palange, and E. Burstein, *Phys. Rev. Lett.* (submitted).

¹⁸K. Nath and A. B. Anderson, *Phys. Rev. B* **38**, 8264 (1988).

¹⁹S. Satpathy and R. M. Martin, *Phys. Rev. B* **39**, 8494 (1989).

²⁰J. E. Northrup, *J. Vac. Sci. Technol. A* **4**, 1404 (1986).